Shot-to-shot consistency of trauma measurements on a BABT rig and Roma Plastilina #1 clay

D. B. Rahbek[1], G. Roberson[2], T. Thorvaldsen[1], A. Wien[2]

[1]Norwegian Defence Research Establishment (FFI), Instituttveien 20, NO-2007 Kjeller, Norway (dennis-bo.rahbek@ffi.no)
[2]NFM Technology, Glynitveien 15, 1400 Ski, Norway

Abstract. NFM Technology and the Norwegian Defence Research Establishment (FFI) are developing a Norwegian test rig for evaluating behind armour blunt trauma, the N-BABT rig. Part of the development process has been selecting a suitable material to use a surrogate chest wall. This membrane needs to exhibit both representative and consistent performance over consecutive impacts while showing minimal part and batch variation. Stereo high-speed cameras were used to capture the dynamic impact on the membranes. These images were analysed using digital image correlation (DIC). The shot-to-shot consistency and printing durability were evaluated using a 144 gram, 62 mm diameter smooth plastic sphere at 48 m/s, with nominally 50 impacts at the centre of each candidate membrane. Within this paper, we present the results of one candidate membrane and a baseline test series using Roma Plastilina clay #1 (RP1). The candidate membrane proved consistent, and the speckle print proved robust for impacts at the same impact point, giving low variations in measurements of maximum membrane displacement (D_{max}), velocity (V_{max}) and viscous criterion (VC_{max})
The membrane displacement was found to be affected by whether the membrane was straight or had a slight bend at the impact point prior to impact, however, neither V_{max} nor VC_{max} was affected by this. All three metrics were found to be sensitive to impact velocity. Normalising for membrane baseline bending and taking impact velocity into account, the shot-to-shot consistency (standard deviation) was as low as 0.9 % for D_{max} and V_{max}, and 2.3 % for VC_{max}. The back-face signature (BFS) values for the RP1 clay were found to correlate with clay temperature in the impact crater, while the sensitivity towards impact velocity was limited. The shot-to-shot consistency was found to be 3.1 % when accounting for temperature and impact velocity. Overall, the N-BABT rig was found to be robust for many consecutive impacts, and this with a very low inherent shot-to-shot variation.

1. INTRODUCTION

Most body armour ballistic test procedures use a witness material (often a modelling clay [1]) to support the body armour and provide a quantification of behind armour trauma, the back-face signature (BFS). BFS is a simple residual static measurement of a dynamic impact and does not accurately address the injury mechanisms of a blunt impact on the body [2]. The widely used Roma Plastilina #1 (RP1) clay is for instance temperature and work sensitive, and its rheological properties might change with time when not being regularly used [3]. The development of the temperature insensitive clay ARTIC [4] solves some of the issues, but it does not allow for capturing the dynamics of the impact event. Moreover, this will not resolve the lab-to-lab and technician-to-technician variability of this style of test procedure, that can affect the outcome of an impact to RP1 and other similar witness materials.

Several behind armour blunt trauma (BABT) rigs have been developed to allow dynamic measurements of impacts on body armour [5-8]. Common for many of these rigs is that they consist of a flexible membrane, made of a silicone or polyurethane, that mimics the response of the torso, i.e. provides a biofidelic response. Some membranes are validated against test on porcine [6], while others against data from tests on post-mortem human subjects (PMHS) [5,7,8]. Depending on the overall rig and set-up, some membranes are cylindrical, whereas others are flat.

There are also variations between the various BABT rigs with respect to the test parameter to be used as injury criteria. Both the membrane velocity and the viscous criterion of the membrane has been utilized. The viscous criterion is used to predict the risk of thorax skeletal injuries and expresses the product of the compression depth and the compression velocity of the torso, adjusted for the chest depth.

As part of the European Defence Agency Category B project CERAMBALL II, NFM Technology and the Norwegian Defence Research Establishment (FFI) have been developing a Norwegian version of a BABT rig, i.e. the N-BABT rig. The aim is to provide more informed advice on injury risk and improved capability to efficiently discern differences between protective materials and armour solutions based on injury criteria metrics.

In this paper, part of the membrane evaluation for the N-BABT rig is presented. The aim with the tests presented here is to evaluate if the properties of the membrane candidates would change as a result of repeated impacts, to assess the inherent variability of membranes and the data capturing methodology, and to compare this with similar tests performed on RP1 clay.

https://doi.org/10.52202/081621-0010

2. EVALUATION OF MEMBRANES

Several polyurethane chemistries and thicknesses have been evaluated in the development of the rig membrane in order to evaluate the stability, performance and endurance of the material and the applied printing method for the speckle pattern needed for the digital image correlation (DIC). The objective is to find a membrane with biofidelic properties, with similar properties as reported by Bir et al. [9] and in STANREC 4744 AEP-99 [10]. Comparisons to the biofidelity criteria in AEP-99 indicates that the membranes are slightly too soft. This will be addressed in next iterations of the set-up.

Three white polyurethane membranes, M30-1, M30-2 and M30-3, were investigated in this work. A speckle pattern was printed on the membrane surface, see Figure 1(b). Several iterations with printing different techniques were needed to obtain a robust print. The speckle print is required to enable the utilisation of DIC, which provides a global noncontact measurement methodology to capture the dynamic impact event. The nominal size of the membranes is 650 mm x 650 mm x 30 mm, with a printed area of 500 mm x 500 mm.

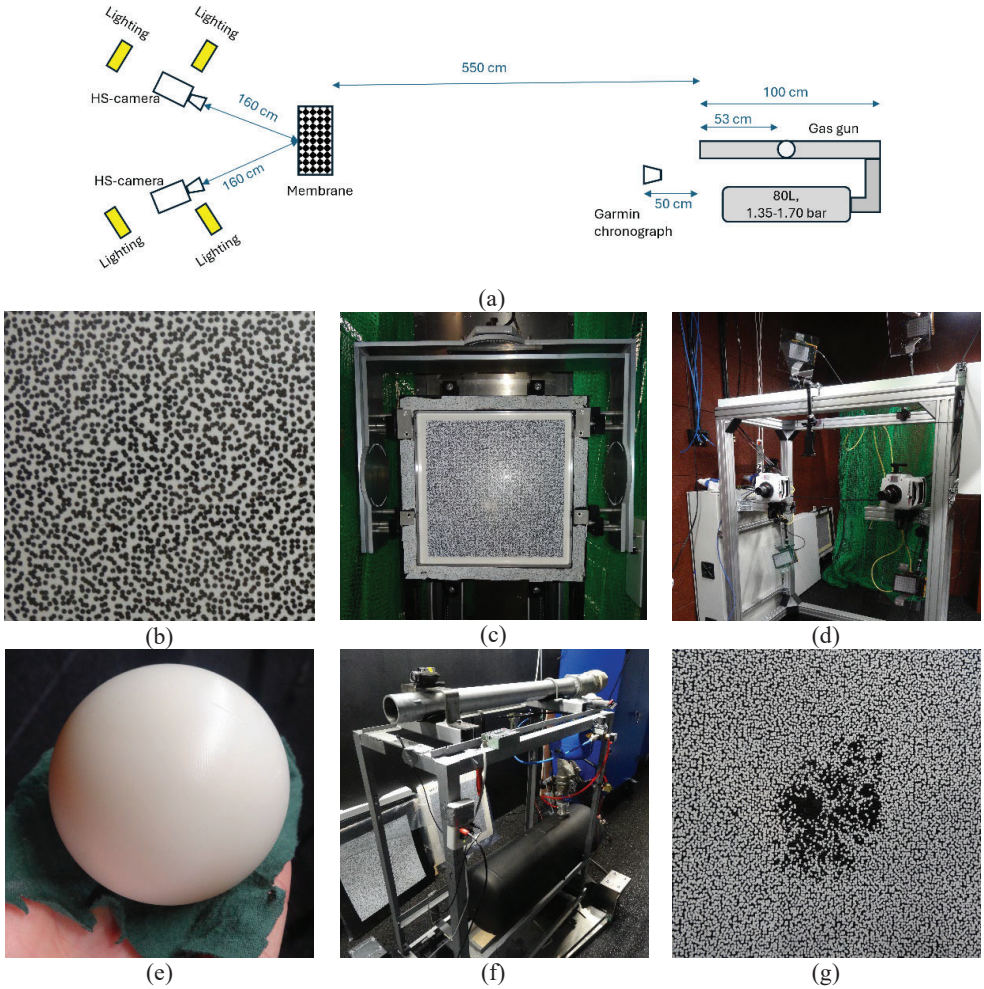

Figure 1. **(a)** The layout of the experimental set-up for the tests on the membranes. The N-BABT rig: (b) speckle print on a membrane, (c) a membrane in the membrane fixture as seen from the camera position, and (d) the frame with two high-speed cameras and four LEDs, (e) nylon ball with cotton gun patch to create a gas seal (f), the gas gun used to propel the nylon ball and (g) an example of damage to a poorly performing print.

3. CURRENT N-BABT SET-UP AND EXPERIMENTAL METHOD

https://doi.org/10.52202/081621-0010

The impact testing on the N-BABT rig was performed at NFM Technology. An overview of the set-up is shown in Figure 1(a). The membrane was clamped in a rigid metal frame, Figure 1(c), which shows the membrane from the camera side. In order to capture the impact event, two high speed cameras, Phantom V2512, were utilized together with four high power LEDs for illumination, Figure 1(d).

To evaluate the inherent properties of the N-BABT rig and the RP1 clay, nylon balls with a diameter of 62 mm and a mass of 144.17 g (with a 0.14 g standard deviation), Figure 1(e), were employed. The desired impact velocity was 48 m/s since the momentum of 6.9 kg·m/s at this velocity is very close to the momentum of 6.8 kg·m/s for the NIJ HG2 threat .44 MAG JHP, 240 grain at 436 m/s, as given in the NIJ Standard 0123.00 [11]. This was expected to give a rather large deformation, which is useful for evaluating if the membrane and print could withstand many impacts. The nylon ball was propelled using a gas gun, shown in Figure 1(f). The velocity was measured using a Garmin Xero C1 Pro radar chronograph. The distance from the gas gun muzzle to the target front, clay or membrane, was 550 cm. Light-screen chronographs were found to be inconsistent and unreliable at low velocities.

3.1 Tests on the N-BABT rig

For the three membranes, the impact position was at the centre position of the membrane. The high-speed cameras were placed 160 cm from the back side of the membrane, Figure 1(a). The cameras resolution was 768 pixels x 768 pixels with a field of view 30 cm x 30 cm around the centre on the "body side" of the membrane. The frame rate was 39100 fps. To find the membrane displacement, all the sets of image pairs were analysed using the VIC-3D DIC software.

The membrane displacement was filtered using a CFC 1000 standard time filter [12], as recommended in the STANREC 4744 AEP-99 [10], and from this the displacement at the impact point, D(t), was found. The membrane velocity, V(t), was found by deriving D(t) with respect to time. Using an average thorax thickness (D0) of 0.236 m, the maximum viscous criterion was computed as explained in [10]

$$VC_{max} = \max((D(t)/D0)*V(t)) \quad (1)$$

An example of the time evolution of the membrane deflection, velocity and viscous criterion of an impact event is presented in Figure 2. The maximum displacement (D_{max}), the maximum velocity (V_{max}) and maximum viscous criterion value (VC_{max}) was then found for each impact event.

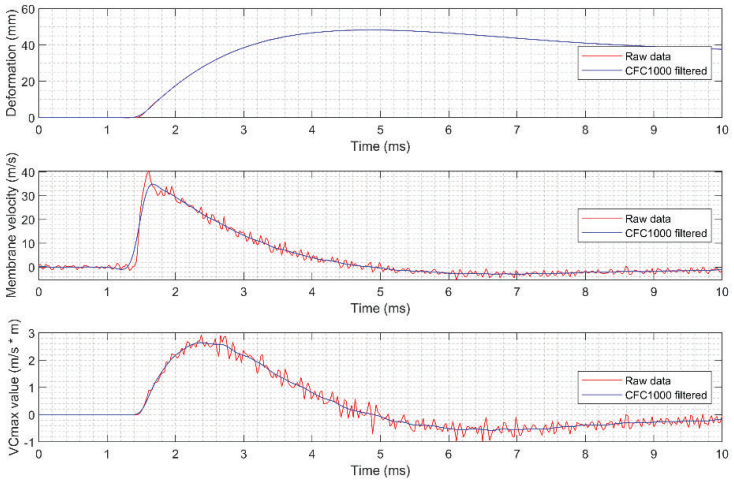

Figure 2. Example of the time evolution of the raw data (red) and the filtered (blue) outcome of an impact on a membrane (not a M30 membrane, but one discarded membrane). Membrane displacement is on top, velocity in the middle and viscous criterion on the bottom. The difference between the raw and filtered data is small for the deformation, but becomes clear when derived with respect to time, as is the case for the velocity.

https://doi.org/10.52202/081621-0010

3.2 Tests on Roma Plastilina No. 1

For the tests on RP1 clay, a test procedure based on the NIJ Standard 0101.06 [1] was applied. Two clay boxes, A and B, were evaluated, both used on almost daily basis. The boxes were kept in an oven and heated to 33 °C. Before use, a drop tests with a 1043 g steel sphere with diameter 63.5 mm was performed. The average drop depth was 18.4 mm for box A, and 20.4 mm for box B.

For the impact testing, the set-up was the same as for the N-BABT, exchanging a clay box for the membrane and without cameras and LED lights. The impact position was in the centre of the clay box. A single 4 ply sheet of soft armour grade ultra-high molecular weight polyethylene (UHMWPE) was placed on the clay before impact, Figure 3(a). This allowed the removal of the ball from the clay without damaging the BFS. Post impact, the UHMWPE sheet and ball were embedded in the clay, Figure 3(b), but was easily removed without disturbing the impact crater, Figure 3(c). Excess clay was scraped off, and the BFS depth was measured using a vernier depth gauge.

Following the measurement of BFS, an infra-red (IR) image was captured of the clay box utilising a FLIR E6 Pro camera. The clay temperature was also measured inside the impact crater at a depth of 10 mm below the surface using a thermocouple thermometer. The clay box was then repaired with clay from the oven, and a new IR image was taken prior to the next test shot. The before and after impact IR images of the clay surface temperature were used to measure the temperature in the crater, which combined with the thermocouple measurements provided an indication of the effects of cooling and locally imparting work into the clay on the BFS. All temperature measurements were performed before adding the UHMWPE layer or after removing the layer. The UHMWPE layer is not expected to affect the temperature of the clay significantly.

(a) (b) (c)

Figure 3. (a) The clay box with the UHMWPE interlayer in position, (b) the ball has impacted the interlayer material and is stuck, and (c) the indentation in the clay after removal of the interlayer.

3.3 Test summary

Table 1 provides an overview of the total number of tests performed for each type of target. There were no velocity readings for the membrane M30-2. Moreover, a number of tests was conducted with the other two membranes, but without velocity readings. The average impact velocities were in the range from 47.2 m/s to 49.1 m/s. The impact velocity was slightly higher for the membrane test, while the standard deviation was slightly lower for the RP1 tests.

Table 1. Overview of the number of tests performed for each type of target.

Type	Target	Accepted tests	Tests with velocity reading	Mean velocity (m/s)	Std. dev. of velocity (m/s)
RP1	Box A	17	17	47.8	0.3
RP1	Box B	38	38	47.2	0.5
Membrane	M30-1	46	39	48.6	1.1
Membrane	M30-2	46	0	-	-
Membrane	M30-3	50	28	49.1	0.6

https://doi.org/10.52202/081621-0010

4. MEMBRANE RESULTS

4.1 Effect of impact number

For the N-BABT rig to be useful for many tests, the membrane performance should not vary significantly during the course of the membrane life. Figure 4 shows the performance for the first 50 impacts. The results for V_{max} and VC_{max} are consistent for all impacts. There are a few impacts with lower values for M30-1, shots 5-10, but this is explained by slightly lower impact velocities, as will be described in section 4.3.

For D_{max}, the results are stable for each individual membrane, especially after around 10-15 shots. The D_{max}, however, appears slightly smaller for the first 10-15 shots. This could possibly be related to the Mullins effect, which describes a softening of elastomers during the first load cycles. Additionally, the displacements on M30-2 are consistently smaller than for the other two, in principle identical, membranes. This was found to be caused by a slight bending of the membrane prior to the impact.

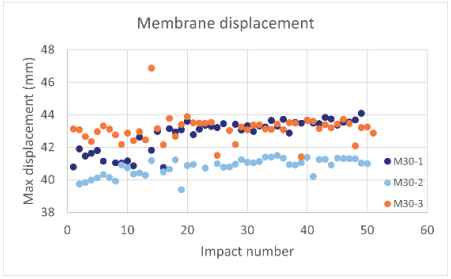

(a)

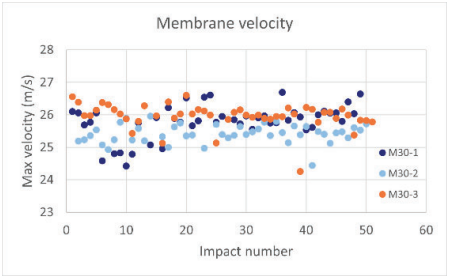

(b)

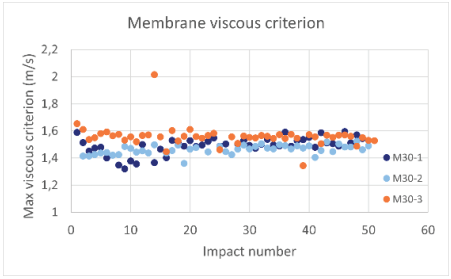

(c)

Figure 4. Results for the three membranes. (a) D_{max}, (b) V_{max}, and (c) VC_{max}.

4.2 Effect of initial membrane position

A metal frame is used to mount and secure the membrane in the test position. When the membrane is fixed in the metal frame, the frame is placed horizontally on a table, and the membrane is placed in the fixture while being supported by the table. This is done in order to keep the membrane as flat as possible with respect to the impact direction, as illustrated in Figure 5(a), where the arrow depicts the Z-plane (out-of-plane direction) of the DIC analysis, as well as the direction of the ball. That is, the membrane deformation is in the positive Z-direction.

It was, however, observed during the data analysis, that there was a slight variation in the starting position of the membrane for the different impacts. The membrane Z-position ranged from roughly -1 mm to -3 mm at impact, Figures 5(b)-(d). This variation in starting position is not due to overall movements of the membrane in the frame, but due to the membrane is beding slightly towards or away from the incoming ball. The negative Z-position means that the membrane is bending slightly towards the incoming nylon ball and away from the cameras, Figure 5(a).

This bending can affect the outcome in two ways. First, the displacement is calculated with the membrane starting position as a zero-point reference. Second, because the initial bending is towards the ball, the membrane can be displaced more with respect to the starting point before it reaches the same level of tension as if the membrane was not bending.

https://doi.org/10.52202/081621-0010

The max displacement and the initial Z-position of the membrane impact point, Figure 5(b), is clearly correlated. This correlation partly explains the slightly smaller displacements observed for the first 10-15 impacts.

For the V_{max} and the VC_{max}, the influence of the initial Z-position appears much smaller. This is likely because both the velocity and the viscous criterion of these measures reach their maximum value long before the max displacement is reached, Figure 2.

In order to assess the influence of the Z-position on the shot-to-shot variation, the data was adjusted for Z-position by fitting a straight line to the data shown in Figures 5(b)-(d) and then adjusting for the slope of this line. The data are presented in Table 2.

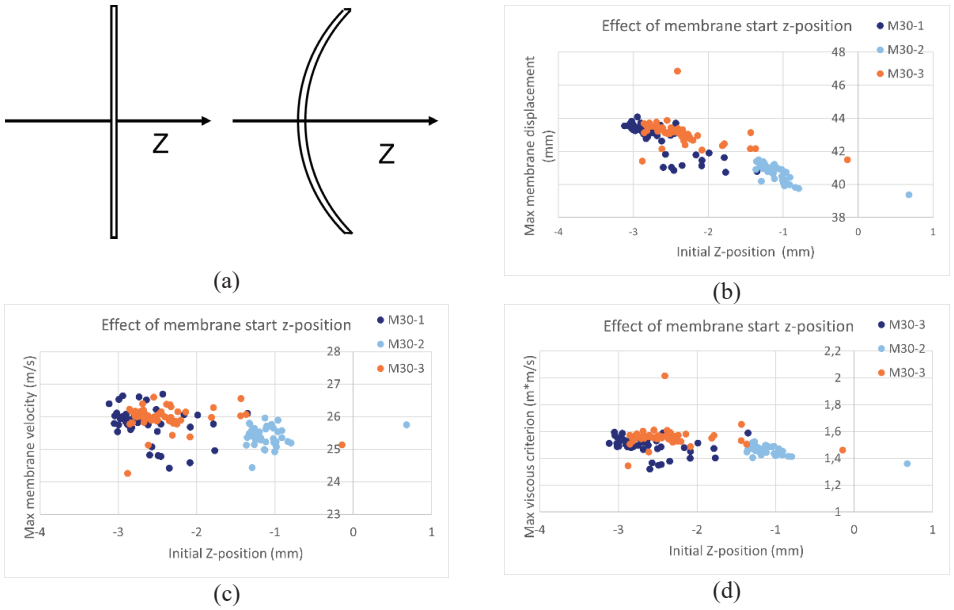

Figure 5. (a) Initial Z-position of the membrane – to the left the membrane is straight and starts in the Z = 0 position, while to the right the membrane is curved against the impact side, and it starts with a negative Z-position. Z-position effect on: (b) D_{max}, (c) V_{max}, (d) VC_{max}.

4.3 Effect of impact velocity

Despite not capturing the impact velocity for all membrane impacts, it is of interest to evaluate how large portion of the shot-to-shot variation arises from the impact velocity variations. In order to evaluate this, the membrane data (adjusted for the initial Z-position, as described in the previous section, and only for the impacts with velocity measurements), have been plotted against the impact velocity in Figures 6(a)-(c).

It is evident from the figures that all the outcome parameters, D_{max}, V_{max} and VC_{max}, correlate with the impact velocity. Given that we want the rig to be sensitive to impact conditions, such as velocity, this is positive. The effect of the velocity on the shot-to-shot variation has been estimated in the same way as for the Z-position, by fitting a straight line to the data and adjusting for the data for the slope. The resulting standard deviations are given in Table 2.

In Table 2, the mean value for D_{max}, V_{max} and VC_{max} are presented for membranes M30-1 and M30-3 for the shots with velocity measurements, and for the two membranes combined as one. The values for the two membranes are very similar for all three measures. From a testing perspective, this is positive since this indicates that it should be possible to compare data from impacts performed on different membranes (that are meant to be identical).

Table 2 also includes the relative standard deviation of the mean, as well as the relative standard deviations when the data are adjusted for the initial Z-position and velocity. Overall, the relative standard deviations are small, from 1.6 % for unadjusted V_{max} to 3.9 % for unadjusted VC_{max}. When adjusted for Z-position, the relative standard deviation drops from 1.9 % to 1.4 % for D_{max}, while the V_{max} and VC_{max} are essentially unaffected. Adjusted for impact velocity the relative standard deviation for both D_{max} and V_{max} is 0.9 %.

https://doi.org/10.52202/081621-0010

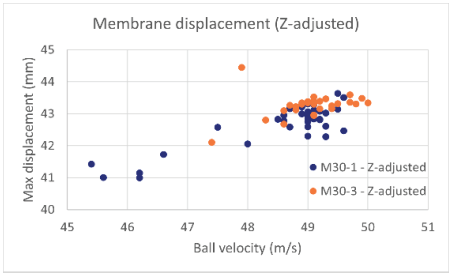

(a)

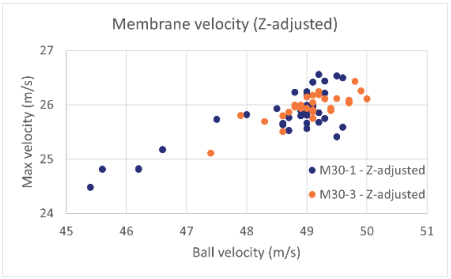

(b)

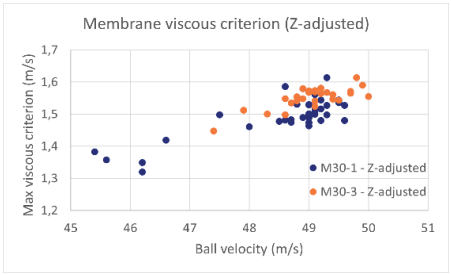

(c)

Figure 6. Effect of ball velocity on the membrane: (a) max displacement, (b) max velocity, (c) VC_{max}.

Table 2. Relative standard deviations for D_{max}, V_{max} and VC_{max} criterion for the membranes, M30-1 and M30-3, with and without adjusting for initial Z-position and impact velocity.

				Z-position adjusted		Z-position and velocity adjusted	
Output	**Membrane**	**Mean**	**Std. dev.**	**Mean**	**Std. dev.**	**Mean**	**Std. dev.**
D_{max}	M30-1	42.8 mm	2.3 %	42.7 mm	1.5 %	42.8 mm	0.8 %
	M30-3	43.1 mm	1.2 %	43.3 mm	0.9 %	43.1 mm	0.9 %
	Combined	**42.9 mm**	**1.9 %**	**42.9 mm**	**1.4 %**	**42.9 mm**	**0.9 %**
V_{max}	M30-1	25.8 m/s	1.9 %	25.8 m/s	1.9 %	25.9 m/s	1.1 %
	M30-3	25.9 m/s	1.1 %	26.0 m/s	1.0 %	25.9 m/s	0.6 %
	Combined	**25.9 m/s**	**1.6 %**	**25.9 m/s**	**1.6 %**	**25.9 m/s**	**0.9 %**
VC_{max}	M30-1	1.49 m/s	4.2 %	1.49 m/s	4.1 %	1.50 m/s	2.4 %
	M30-3	1.55 m/s	2.3 %	1.55 m/s	2.1 %	1.54 m/s	1.4 %
	Combined	**1.52 m/s**	**3.9 %**	**1.52 m/s**	**3.9 %**	**1.52 m/s**	**2.3 %**

5. ROMA PLASTILINA RESULTS

5.1 Effect of impact number

The BFS values for the impacts are presented in Figure 7. The BFS values are scattered around 48 mm, from roughly 44 mm to 52 mm. The BFS for the two clay boxes appear to be similar. This means that tests performed with body armour on the two clay boxes can be compared. There does not appear to be a clear trend for the BFS with respect to impact number. One concern is that the clay temperature would change during the testing, as the laboratory room temperature is below the oven temperature. However, given that the impact position was the same for all shots, and that new clay from the oven was used to fill the crater, the temperature was fairly stable in that region during testing.

https://doi.org/10.52202/081621-0010

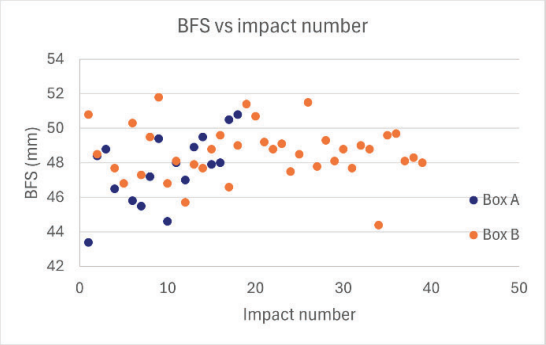

Figure 7. BFS values as function of impact number for the two clay boxes, A and B.

5.2 Effect of clay temperature

Of the measured temperature data, the BFS and the IR-based surface temperature after impact showed the highest degree of correlation (the trends were the same for the other measures).

Figure 8(a) shows the BFS values as a function of the clay surface temperature after impact for both clay boxes. The temperature span was larger for box A than for box B. This is most likely explained by the fact that box A was used in the first tests, and that the measurement routines were more established for box B. The test frequency was around 7 min for box A and 5 min for box B. The data show that the BFS is higher when the clay temperature after testing is higher. It is also clear that the BFS varies for the same temperature.

The RP1 BFS data have been adjusted for temperature by fitting a straight line to the data and adjusting for the slope. The relative standard deviations are given in Table 3.

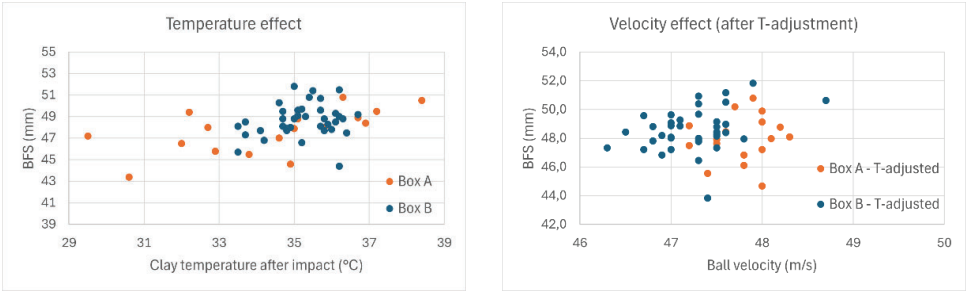

(a) (b)

Figure 8. (a) BFS values as a function of temperature inside the impact crater after impact and (b) BFS values (adjusted for clay temperature) as a function of impact velocity.

5.3 Effect of impact velocity

The effect of impact velocity on the BFS values (temperature-adjusted) are shown in Figure 8(b). There is a slight tendency towards higher BFS values for higher velocities, but the data scatter for identical impact velocities is large compared to the variation in impact velocity, 0.7 % and 1.0 % for box A and B (based on Table 1), respectively.

The results in Table 3 show that the mean BFS values for the two boxes are not very different, as Figure 7 also showed. The relative standard deviation for the unadjusted data was quite low, 4.2 % and 3.2 % for box A and B (on the order of 1.5-2.0 mm for the measured BFS values). When adjusted for the temperature, the relative standard deviation became lower for box A, where the temperature ranges were the largest, while there was no substantial effect for box B. The adjustment for impact velocity only lowers the relative standard deviation slightly, which means that for these tests, the temperature and impact velocity was well controlled, and that the inherent shot-to-shot variation was on the order of 3 %. It is worth noting here, that the use of the UHMWPE layer placed on the clay box for making ball extraction easier could have contributed to the variation from shot-to-shot.

https://doi.org/10.52202/081621-0010

Table 3. BFS results both with and without adjusting for clay temperature and impact velocity.

	BFS		Temperature adjusted BFS		Temperature and velocity adjusted BFS	
Clay box	**Mean**	**Std. dev.**	**Mean**	**Std. dev.**	**Mean**	**Std. dev.**
Box A	47,7 mm	4,2 %	48.0 mm	3.4 %	47.7 mm	3.4 %
Box B	48.6 mm	3.2 %	48.5 mm	3.1 %	48.6 mm	2.9 %
Combined	**48.3 mm**	**3.6 %**	**48.4 mm**	**3.2 %**	**48.3 mm**	**3.1 %**

6. DISCUSSION

The data from the membrane and the RP1 clay testing is summarised in Figure 9. The relative standard deviations for the combined data for the RP1 and for the membranes are compared with and without adjusting for temperature/Z-position and impact velocity. The data shows that the shot-to-shot variation of the membrane are lowest for D_{max} and V_{max}. It is roughly half of the clay variation and the VC_{max} variation. The higher VC_{max} variation is not surprising since it is the product of the other two measures. The shot-to-shot variation of VC_{max} and the RP1 clay is similar. The VC_{max} value was essentially insensitive to variation in the initial Z-position (bending) of the membrane, something that could prove problematic from an experimental point of view if it had. We do not plan on correcting for initial Z-position in the future.

Moreover, the VC_{max} was found to be velocity sensitive, which is not surprising since it is the product of the velocity and the displacement, which were both found to be velocity sensitive. Given that the VC_{max} value is the value that is meant to inform about the risk of injury, it is positive that the shot-to-shot variation of this parameter is comparable to the existing test method, RP1 clay, if not even slightly better.

For further analysis, it would be interesting to compare the correlation between D_{max}, V_{max} and VC_{max} for identical impacts. If the correlation is strong, then for instance the V_{max} value, which has low Z-position sensitivity and displays a low shot-to-shot variation, might be a useful measure in for instance product development, where a small variation would allow for more accurate measurement with fewer shots.

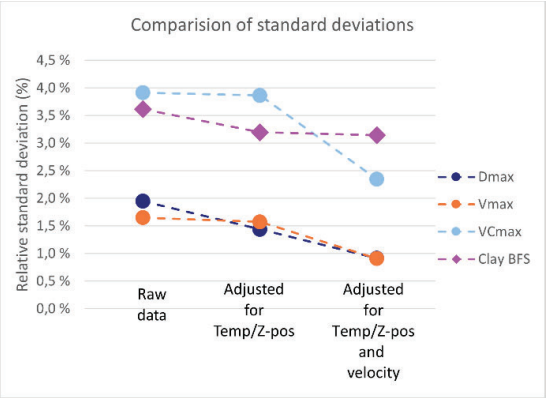

Figure 9. Relative standard deviations for the membrane data: D_{max}, V_{max}, VC_{max} compared with clay BFS. The raw data are compared to the data adjusted for temperature/Z-position and velocity.

7. CONCLUSION

The current state of the N-BABT rig has been described together with experimental tests performed to evaluate the endurance and inherent variation of the rig. The main objective with the testing was to evaluate 1) whether the selected membrane material would give consistent results for a substantial number of impacts, 2) if the three tested and "identical" membranes would yield identical results, and 3) that the variation from shot-to-shot was not inferior to the commonly used clay witness material, i.e. Roma Plastilina #1.

https://doi.org/10.52202/081621-0010

The results showed that the membrane-to-membrane variation was small, that the membranes showed an overall low shot-to-shot variability with respect to all measures, D_{max}, V_{max} and VC_{max}, with relative standard deviations of 1.9 %, 1.6 % and 3.9 %, respectively. For the RP1 clay the value was 3.6 %. It was also observed that the initial position of the membrane (caused by bending of the membrane) had a substantial effect on the measured D_{max}, but not on V_{max} and VC_{max}. When the data was adjusted for initial membrane bending and impact velocity, to assess the inherent variability, the relative standard deviations for the measures from the membrane was 0.9 %, 0.9 % and 2.3 % for D_{max}, V_{max} and VC_{max}, respectively. For the RP1 clay, the adjustment with respect to clay temperature and impact velocity resulted in an estimate for the inherent relative standard deviation of 3.1 %.

Acknowledgments
The authors would like to acknowledge Rune Mellem, Sondre Gabrielsen and August B. Strengen, NFM Technology, for their assistance during the experiments. Susanne Thomesen and Toivo Horvei, NFM Technology, are thanked for valuable comments and discussions, and Bernt B. Johnsen, FFI, is acknowledged for proofreading the manuscript.

References

[1] NIJ Standard 0101.06, Ballistic Resistance of Body Armor, National Institute of Justice, July 2008.
[2] Cannon L., Behind Armour Blunt Trauma - an emerging problem, J R Army Med Corps, 147 (2001), 87-96.
[3] Gardner J., Cora Cruz J., Mrozek R., Hopping J., Beaudoin E., Lombardo L., Ballistic Assessments of the ARL Reusable Temperature Insensitive Clay (ARTIC) as a Ballistic Backing Material, Proceedings of the Personal Armour Systems Symposium, Dresden, Germany, 2023, pp. 208-217.
[4] Roberson C., Perciballi W., Rogers D., Fleming D., Consistently Depressed?, Personal Armour Systems Symposium, Quebec, Canada, 2010
[5] Anctil, B., Bayne, T., Bourget, D., Pageau, G., Binette, J.-S., Rice, K., and Toman, A., An Alternative to Plastilina for Evaluating the Performance of Body Armours, Personal Armour Systems Symposium, Brussels, Belgium, 2008.
[6] Tam, W., Rozant, O., Thoral-Pierre, K., Pope, D., Softley, I., Baker, L., Cook, W., Scaramuzzino, P., and Ferry, E. The UK Behind Armour Blunt Trauma Rig – 20 years on, Proceedings of the Personal Armour Systems Symposium, Amsterdam, Netherlands, 2016.
[7] Andrei A., Robbe C., Penders, T., Papy, A., Development of a new thoracic surrogate for KENLW and BABT impacts, Proceedings of the Personal Armour Systems Symposium, Dresden, Germany, 2023, pp. 321-340.
[8] N. Shewchenko, E. Fournier, T. Bayne, S. Magnan, and D. Bourget, The Development of the f-BTTR and its use for Hard Armour Testing, Proceedings of Personal Armour Systems Symposium, Copenhagen, Denmark, 2020, pp. 481-490.
[9] Bir C., Viano D., King A., Development of biomechanical response corridors of the thorax to blunt ballistic impacts, J. Biomech, 37 (2204), 73-79.
[10] NATO, STANREC 4744 edition 5 - AEP 99 ed: b ver 1, Thorax injury risk assessment of non-lethal projectiles, 2021.
[11] NIJ Standard 0123.00, Specification for NIJ Ballistic Protection Levels and Associated Test Threats, National Institute of Justice, October 2023.
[12] SAE, Part 1 - Electronic Instrumentation, in Surface Vehicle Recommended Practice, SAE-J211-1 Instrumentation for Impact Test, Warrendale, PA, USA, The Engineering Society For Advancing Mobility Land Sea Air and Space International, 1995.

https://doi.org/10.52202/081621-0010